Tunable High-Intensity Electron Bunch Train Production Based on Nonlinear Longitudinal Space Charge Oscillation

Zhen Zhang,[1] Lixin Yan,[1] Yingchao Du,[1] Zheng Zhou,[1] Xiaolu Su,[1] Lianmin Zheng,[1] Dong Wang,[1] Qili Tian,[1] Wei Wang,[1] Jiaru Shi,[1] Huaibi Chen,[1] Wenhui Huang,[1] Wei Gai,[1,2] and Chuanxiang Tang[1,*]

[1]*Department of Engineering Physics, Tsinghua University, Beijing 100084, China*

[2]*Argonne National Laboratory, Lemont, Illinois 60439, USA*

(Received 23 February 2016; published 5 May 2016)

High-intensity trains of electron bunches with tunable picosecond spacing are produced and measured experimentally with the goal of generating terahertz (THz) radiation. By imposing an initial density modulation on a relativistic electron beam and controlling the charge density over the beam propagation, density spikes of several-hundred-ampere peak current in the temporal profile, which are several times higher than the initial amplitudes, have been observed for the first time. We also demonstrate that the periodic spacing of the bunch train can be varied continuously either by tuning launching phase of a radio-frequency gun or by tuning the compression of a downstream magnetic chicane. Narrow-band coherent THz radiation from the bunch train was also measured with μJ-level energies and tunable central frequency of the spectrum in the range of ~0.5 to 1.6 THz. Our results pave the way towards generating mJ-level narrow-band coherent THz radiation and driving high-gradient wakefield-based acceleration.

DOI: 10.1103/PhysRevLett.116.184801

In recent years there has been great interest in the generation and control of high frequency structures in the longitudinal distribution of relativistic electron beams. Bunch trains, consisting of a large number of equally spaced electron microbunches, have been considered for the resonant excitation of the wakefields in plasma and dielectric wakefield accelerators [1–7], and for production of beam-based high power, narrow-band radiation in the terahertz (THz) spectral range [8–10].

Typically, the wakefield-based acceleration is driven by a single electron bunch. One way to increase the accelerating gradient is using the bunch train with the spacing matching the wakefield wavelength, where the wakefield is linear superposition according to the number of bunches [3–6]. The method has been used in the dielectric wakefield accelerator with centimeter spacing [7]. However, it is still challenging to produce bunch train for the plasma wakefield acceleration as the plasma wavelength typically is of the order of a few tens or hundreds of microns. In addition, tunable coherent THz radiation with a narrow spectral bandwidth is of great interest for molecular spectroscopy, resonant control, and imaging [11–13]. While there are a variety of techniques developed to generate narrow-band THz radiation (e.g., Refs. [14–16]), electron bunch train is a promising media with great potentials to produce intense narrow-band THz radiation.

Several methods have been proposed and studied to generate ps and sub-ps spaced bunch trains. These include the conversion of transverse modulation into a periodic longitudinal distribution with the use of dispersive beam line and initial energy chirp [17], or the emittance-exchange technique [18]. The generation of transverse modulation using a mask will always lead to particle loss. Another possibility is to introduce an energy modulation by self-excited wakefields [19,20] and then convert it to density modulation through a magnetic chicane [21]. The difference-frequency method based on the electron-laser interaction [22,23] can be also used to generate THz structures although the implementation will be slightly more complex. In addition, many authors have proposed a straightforward method, imposing modulation on the beam directly at the cathode and trying to maintain it as the beam propagates [10,24,25]. This method suffers from the smearing effect of longitudinal space charge forces and the initial modulation might blur and tend to disappear for large beam currents. Some improved methods have been considered to compensate this effect and recover the initial modulation [26,27].

As opposed to trying to reduce the effect of longitudinal space charge forces, Musumeci *et al.* proposed to take advantage of it to magnify the initial density modulation through strengthening the space charge forces and letting the beam distribution evolve in the nonlinear regime [28]. A proof-of-principle experiment with a few pC beam charge (up to ~20 pC) was carried out a few years ago [28] and this scheme was proposed to generate high peak current bunch trains [29]. For a large enough initial density modulation, the linear theory, which predicts a periodic evolution of the beam density with the periodicity set by the relativistic plasma frequency, breaks down and the dynamics is more complicated due to the appearance of harmonics of the modulation frequency along the beam propagation. The harmonics interfere constructively after $1/2$ plasma oscillation period (π phase advance) leading to the formation of high peak current spikes. The evolution of the

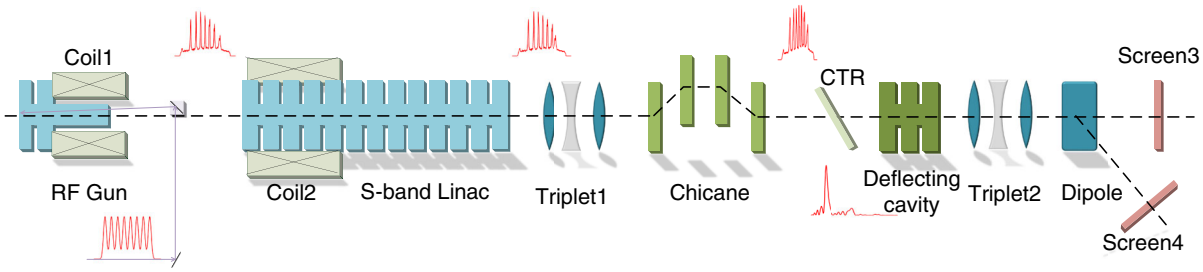

FIG. 1. Schematic layout of the beam line for bunch train generation (not to scale). The inset plots are the longitudinal profile of the laser and electron beams, and the THz spectrum. The deflecting cavity is used to streak a portion of the beam across a luminescent screen to measure the beam's longitudinal profile.

electron beam in the nonlinear regime can be well formulated using the 1D cold fluid model [28,29].

In this Letter, we explore experimentally the possibility of using this technique to generate ps spaced bunch trains with large charge and high peak currents. The experiment was performed at the Tsinghua Thomson scattering x-ray source [30]. A schematic of the experiment is presented in Fig. 1. The cathode in a 1.6 cell rf photoinjector is illuminated by a train of 8 equally spaced laser pulses created using 3α-BBO birefringent crystals [31–34] of thickness 5.68, 2.84, and 1.42 mm, respectively. The induced separation between neighboring pulses is 1 ps with frequency content of 1 THz. The beam charge after the crystals can be varied from a few pC up to ~1 nC. By optimizing the laser spot on cathode and the solenoid focusing after the gun, we can control the plasma frequency of the longitudinal oscillation before the beam enters the acceleration section where it will be quickly accelerated to ~45 MeV to freeze its longitudinal structure. The beam modulation can be observed directly by an rf deflector and can also be confirmed by the measurement of the autocorrelation function of coherent transition radiation (CTR) produced when the beam passes through a foil.

A typical measurement of the bunch train with high beam charge by the deflector (~700 pC) is presented in Fig. 2. The laser spot on the cathode was optimized to be ~4 mm in diameter and the full width at half maximum (FWHM) of the single laser pulse before stacking was ~500 fs. The phase of the gun was set at 30° with maximum acceleration gradient 106 MV/m. The gun solenoid was set to 2230 Gs and linac solenoid was ~800 Gs. The acceleration section was set at on-crest and the chicane was turned off. For a large beam charge, as the beam experiences strong focusing at low energy, it is difficult to get very small unstreaked beam size by using the current focusing system in the beam line, which limits the temporal resolution of the deflector. In order to resolve the temporal profile, we implemented a 70-μm horizontal slit before the deflector to cut the beam transversely and so that a small fraction of charge could be streaked. We varied the position of the slit and the measured distributions were similar. We observed 7 bunches with ~250 A peak current (150 A for the head subbunch) and ~1 ps periodic spacing. Compared with the initial modulation (peak current ~130 A), the modulation is enhanced by the longitudinal space charge forces.

The beam charge and the solenoid focusing were also varied to control the electron beam density along the propagation so that we can observe the process of oscillation and the evolution of the beam longitudinal profile, as shown in Fig. 3. Their oscillation phase advances Φ are also given in the figures, which characterizes the plasma oscillation and can be calculated in terms of the 3D plasma frequency ω_{p3D} [28]. In order to characterize the modulation in the temporal profile, we introduce the bunching factor $b(k) = \int I(t)e^{-ikct}dt/\int I(t)dt$, where k is the wave number, $I(t)$ is the current profile along the longitudinal coordinate t, and c is the speed of light. We perform fully 3D particle tracking simulations with the GENERAL PARTICLE TRACER (GPT) code [35] using different experimental parameters to obtain the plasma frequency along the propagation and the corresponding bunching factor, as presented in Fig. 3(e). When the phase advance approaches $\Phi/2\pi \approx 0.25$, the density modulation reaches a minimum. Increasing it close to π after this, the modulation

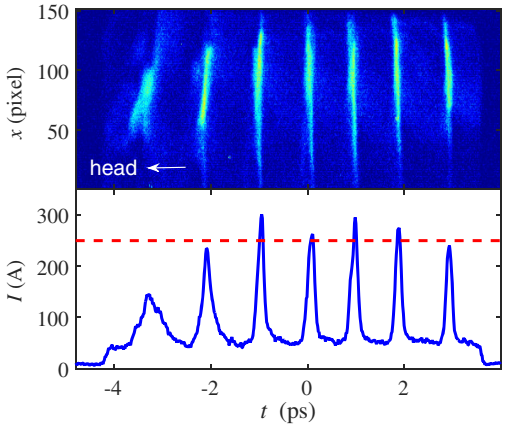

FIG. 2. Measured longitudinal distribution (top) and projected density profile (bottom) of the bunch train with a horizontal slit before the deflector.

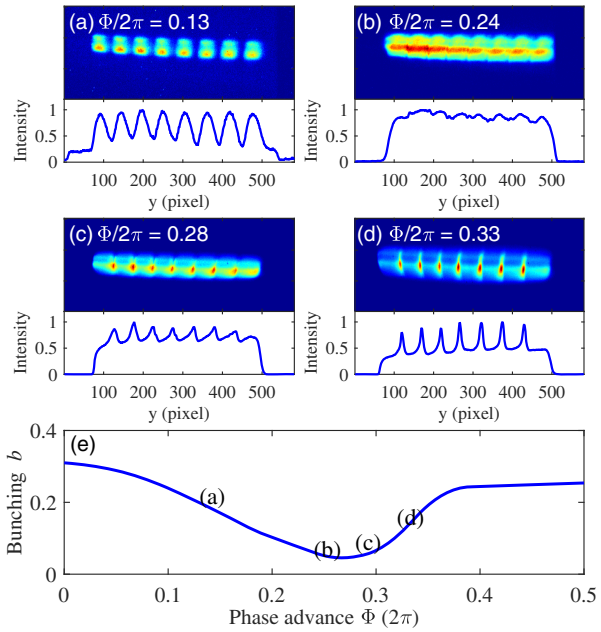

FIG. 3. (a)–(d) Streak images and temporal profiles for four different plasma oscillation phase advances. (e) Simulated dependence of the final bunching on the phase advance. Bunch head lies to the left.

reappears and 7 narrow current spikes arise from the valleys of the original 8 peaks.

The modulation in the temporal profile was confirmed by the CTR radiation from the beam. We analyzed the time structure of the signal with a Michelson interferometer using a Golay cell as the detector (not shown in Fig. 1) that characterizes the periodicity of the electron bunch. A typical autocorrelation function is shown in Fig. 4. With the dc offset subtracted, the Fourier transform of the autocorrelation function gives the power spectrum of the THz radiation, also shown in Fig. 4. The central frequency

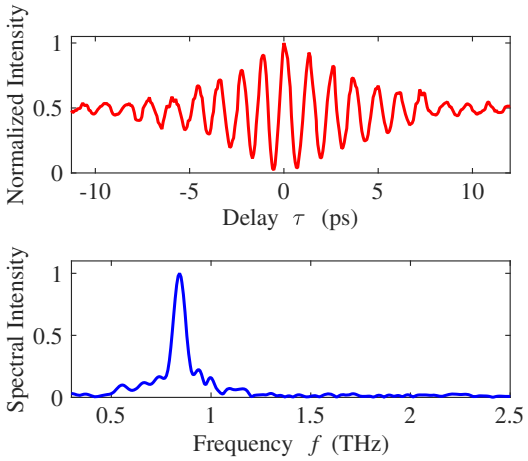

FIG. 4. Normalized autocorrelation function of the CTR THz radiation (top) and the THz spectrum (bottom). The central frequency of the spectrum is ∼0.85 THz as the launching phase of the gun is 40°.

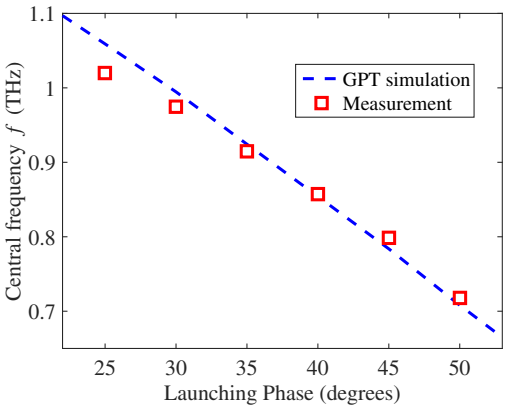

FIG. 5. Central frequency of the THz radiation as a function of the launching phase in the gun.

of the spectrum, corresponding to the average spacing of the bunch train, is ∼0.85 THz since the launching phase in the gun of the electron beam was set at 40° for this measurement. A train of N electron bunches results in an interferogram with $2N-1$ peaks. The number of peaks of the autocorrelation function is 13, in agreement with the expected 7 bunches.

One could control the central frequency of the CTR radiation by changing the launching phases, which influence the overall bunch compression or stretching due to the velocity bunching. The results of experimental measurements and GPT simulations are presented in Fig. 5. In these measurements, the acceleration section was set at maximum acceleration. By changing the launching phase from 50° to 25°, we observed the central frequency changing from ∼0.7 to ∼1 THz, which agrees very well with the GPT simulations.

The central frequency can be varied continuously by the chicane as well. If the electron beam was accelerated off-crest to induce an energy chirp, the central frequency of the radiation spectrum would be a function of the chicane current. The measurement results are shown in Fig. 6 with

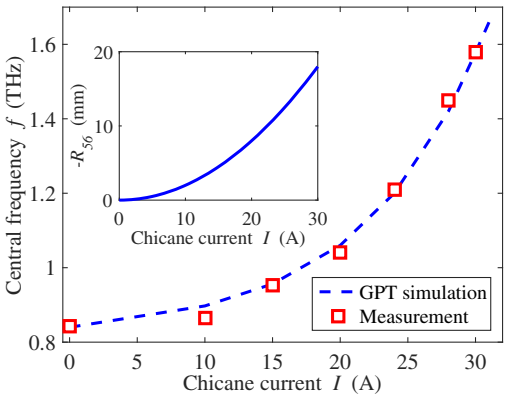

FIG. 6. Central frequency of the THz radiation as a function of the chicane current. The inset shows the R_{56} of the chicane for different exciting currents.

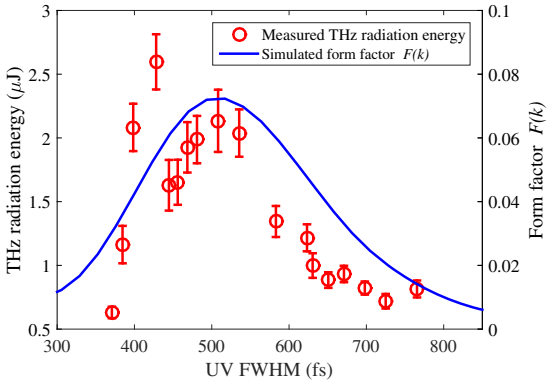

FIG. 7. THz radiation energy averaged over 100 shots for different single UV laser FWHMs before stacking. The blue curve is the simulated form factors. The central frequency is fixed at ~0.85 THz.

−37° off-crest phase. The launching phase of the electron beam was fixed at 45° during the measurements. The inset gives the corresponding R_{56} of the chicane for different exciting currents. In the experiment, the central frequency was increased by a factor of 2 by the bunch compression. If we compress the bunch further, the nonlinear effect in the compression will make the bunch train nonuniform and lead to poor spectral properties. A large R_{56} of the chicane will also reduce the bunching factor quickly as there is some additional local energy chirp on the beam developed from the space charge forces where the current spikes arise. In addition to compressing the bunch, we can also stretch it to decrease the central frequency. The frequency range of the CTR radiation obtained in the experiment was from ~0.5 to ~1.6 THz, which means the average spacing of the bunch train was from ~0.6 to ~2 ps.

In addition to the spectral properties, we also optimized the total THz energy of the CTR radiation by varying the single ultraviolet (UV) pulse width. In the experiment, the UV pulse width was changed by tuning the infrared compressing grating before the third harmonic generation process and measured by the cross-correlation technique with an infrared laser. For a fixed 1-ps periodic spacing, different single UV widths lead to different initial modulation depth. Figure 7 presents the measurements of THz energy by a calibrated Golay cell at different UV FWHMs. The launching phase was set at 40° and the chicane was turn off. We also show the simulated form factor $F(k) = |b(k)|^2$ at the same parameters for comparison in the figure. In principle the THz radiation energy is proportional to the form factor. Both measurements and simulations show that the optical UV FWHM is around 500 fs. The corresponding THz radiation energy obtained in the experiment is ~2 μJ.

In summary, we have observed high-charge high peak current electron bunch trains based on the nonlinear longitudinal space charge oscillation, orders of magnitude higher than previous results. We imposed a ps initial modulation on the beam at the cathode and controlled its oscillation phase advance over the propagation by the external focusing. The bunch train was measured both by a deflector directly and CTR radiation. The peak current of the current spikes in the temporal profile was up to ~250 A, enhanced by a factor of 2 compared with the initial modulation. Narrow-band coherent THz radiation was also generated from the bunch trains. The central frequency of the radiation spectrum can be varied continuously by the overall bunch compression or stretching. The frequency range achieved in the experiment was from ~0.5 to ~1.6 THz. We also measured the THz energy of the CTR radiation for different UV pulse widths. The optimized pulse energy in the measurements is ~2 μJ with ~500 fs FWHM of single UV pulse. If we apply the bunch train to dielectric tubes, mJ-level pulse radiation energy will be achievable [21]. For example, using a 30-mm long quartz tube of outer (inner) diameter 0.4 (0.3) mm, the radiation power is ~8 MW and pulse energy ~1.4 mJ at 0.7 THz. This kind of THz source will open up new opportunities to study material spectroscopy and characterization [36] and THz-driven particle acceleration [37].

The authors want to thank R. K. Li from SLAC for many helpful discussions and suggestions on the experiment. This work was supported by the National Natural Science Foundation of China (NSFC Grants No. 11475097, No. 11375097, and No. 11435015) and the National Key Scientific Instrument and Equipment Development Project of China (Grant No. 2013YQ12034504).

*tang.xuh@tsinghua.edu.cn

[1] I. Blumenfeld *et al.*, Nature (London) **445**, 741 (2007).
[2] M. Litos *et al.*, Nature (London) **515**, 92 (2014).
[3] P. Chen, J. M. Dawson, R. W. Huff, and T. Katsouleas, Phys. Rev. Lett. **54**, 693 (1985).
[4] R. D. Ruth, P. L. Morton, P. B. Wilson, and A. W. Chao, Part. Accel. **17**, 171 (1985); Report No. SLAC-PUB-3374.
[5] P. Schutt, T. Weiland, and V. M. Tsakanov, in *Proceedings of the Second All-Union Conference on New Methods of Charged Particle Acceleration* (Springer, New York, 1989).
[6] J. G. Power, W. Gai, X. Sun, and A. Kanareykin, *Proceedings of the 2001 Particle Accelerator Conference*, PAC 2001 (IEEE, Bellingham, WA, 2001), Vol. 1, pp. 114–116.
[7] C. Jing, A. Kanareykin, J. G. Power, M. Conde, Z. Yusof, P. Schoessow, and W. Gai, Phys. Rev. Lett. **98**, 144801 (2007).
[8] G. L. Carr, M. C. Martin, W. R. McKinney, K. Jordan, G. R. Neil, and G. P. Williams, Nature (London) **420**, 153 (2002).
[9] A. Gover, Phys. Rev. ST Accel. Beams **8**, 030701 (2005).
[10] Y. Shen, X. Yang, G. L. Carr, Y. Hidaka, J. B. Murphy, and X. Wang, Phys. Rev. Lett. **107**, 204801 (2011).
[11] P. H. Siegel, IEEE Trans. Microwave Theory Tech. **50**, 910 (2002).
[12] M. Liu *et al.*, Nature (London) **487**, 345 (2012).
[13] T. Kampfrath, K. Tanaka, and K. A. Nelson, Nat. Photonics **7**, 680 (2013).

[14] A. S. Weling, B. B. Hu, N. M. Froberg, and D. H. Auston, Appl. Phys. Lett. **64**, 137 (1994).
[15] J. Y. Sohn, Y. H. Ahn, D. J. Park, E. Oh, and D. S. Kim, Appl. Phys. Lett. **81**, 13 (2002).
[16] S. Bielawski *et al.*, Nat. Phys. **4**, 390 (2008).
[17] P. Muggli, V. Yakimenko, M. Babzien, E. Kallos, and K. P. Kusche, Phys. Rev. Lett. **101**, 054801 (2008).
[18] Y.-E Sun, P. Piot, A. Johnson, A. H. Lumpkin, T. J. Maxwell, J. Ruan, and R. Thurman-Keup, Phys. Rev. Lett. **105**, 234801 (2010).
[19] S. Antipov, C. Jing, M. Fedurin, W. Gai, A. Kanareykin, K. Kusche, P. Schoessow, V. Yakimenko, and A. Zholents, Phys. Rev. Lett. **108**, 144801 (2012).
[20] K. Bane and G. Stupakov, Nucl. Instrum. Methods Phys. Res., Sect. A **677**, 67 (2012).
[21] S. Antipov, M. Babzien, C. Jing, M. Fedurin, W. Gai, A. Kanareykin, K. Kusche, V. Yakimenko, and A. Zholents, Phys. Rev. Lett. **111**, 134802 (2013).
[22] D. Xiang and G. Stupakov, Phys. Rev. ST Accel. Beams **12**, 080701 (2009).
[23] M. Dunning *et al.*, Phys. Rev. Lett. **109**, 074801 (2012).
[24] Y. Li and K. J. Kim, Appl. Phys. Lett. **92**, 014101 (2008).
[25] J. G. Neumann, R. B. Fiorito, P. G. O'Shea, H. Loos, B. Sheehy, Y. Shen, and Z. Wu, J. Appl. Phys. **105**, 053304 (2009).
[26] M. Boscolo, M. Ferrario, I. Boscolo, F. Castelli, and S. Cialdi, Nucl. Instrum. Methods Phys. Res., Sect. A **577**, 409 (2007).
[27] E. Chiadroni *et al.*, Rev. Sci. Instrum. **84**, 022703 (2013).
[28] P. Musumeci, R. K. Li, and A. Marinelli, Phys. Rev. Lett. **106**, 184801 (2011).
[29] P. Musumeci, R. K. Li, K. G. Roberts, and E. Chiadroni, Phys. Rev. ST Accel. Beams **16**, 100701 (2013).
[30] Y. C. Du, L. Yan, J. Hua, Q. Du, Z. Zhang, R. Li, H. Qian, W. Huang, H. Chen, and C. Tang, Rev. Sci. Instrum. **84**, 053301 (2013).
[31] J. Power and C. Jing, AIP Conf. Proc. **1086**, 689 (2009).
[32] L. X. Yan *et al.*, *Proceedings of the 1st International Particle Accelerator Conference (IPAC)* (IPAC, Kyoto, Japan, 2010).
[33] P. Musumeci, J. T. Moody, C. M. Scoby, M. S. Gutierrez, M. Westfall, and R. K. Li, J. Appl. Phys. **108**, 114513 (2010).
[34] L. X. Yan, J.-F. Hua, Y.-C. Du, Y.-F. Huang, Y. You, D. Wang, W.-H. Huang, and C.-X. Tang, J. Plasma Phys. **78**, 429 (2012).
[35] http://www.pulsar.nl/gpt.
[36] B. Ferguson and X. C. Zhang, Nat. Mater. **1**, 26 (2002).
[37] E. A. Nanni, W. R. Huang, K.-H. Hong, K. Ravi, A. Fallahi, G. Moriena, R. J. Dwayne Miller, and F. X. Kärtner, Nat. Commun. **6**, 8486 (2015).